Analytical Longitudinal Speed Planning For CAVs with Previewed Road Geometry and Friction Constraints*

Liming Gao, Craig Beal, Daniel Fescenmyer, Sean Brennan, *IEEE Member*

***Abstract*— Due to the lack of information, current vehicle control systems generally assume that the friction ahead of a vehicle is unchanged relative to the vehicle's position. However, with connectivity either to other vehicles, infrastructure, or cloud services, future vehicles may have access to this information which is particularly valuable for planning velocity trajectories ahead. This work introduces a method for planning longitudinal speed profiles for Connected and Autonomous Vehicles (CAVs) that have previewed information about road geometry and friction conditions. The novelty of this approach is to explicitly include consideration of the friction ellipse available to the vehicle to develop an analytical solution to the allowable velocity profile that prevents departure from the friction ellipse. The results further define the relationship between the minimum preview distance and longitudinal velocity limits that ensure the vehicle has sufficient time to take action for upcoming hazardous situations. The efficacy of the algorithm is demonstrated through an application case where a vehicle is navigating curvy roads with changing friction conditions at maximum speeds, with results showing that the vehicle consistently operates within the available friction limits.**

I. Introduction

The traffic accident is fatal and has a huge negative influence on economic costs. [follow some data from reference] Many factors attribute to the accident, but a large part of them is caused by slick road conditions (snow, ice, raining, etc.) or over speeding. (make it positive: maximize the mobility throughout the highway system in any condition)

One way to make cars safer is the development of the ADASs (Advanced Driver Assistance Systems) such as EBS, LKA, and ESC, etc., which can assist the driver to follow the desired path stably in hazardous situations. The assistance system can be categorized into lateral control, longitudinal control, and hybrid control. The controller can output proper steering angle and/or driving/braking torque command once the vehicle is out of stability. For example, Yu, et al. [1] designed a feedback-feedforward steering controller to improve the vehicle stability when hard-braking maneuvers on road with split friction. Li, et al. presented a torque control strategy for the situation of abrupt changes in the road friction [2].

However, most of the controllers are activated only when the vehicle states have a significant deviation from the nominal value. Additionally, the controller has a stable region. Consequently, the controller even fails to keep the vehicle stable if the road condition changes intensively. [ref]

Different from the reaction controller, researchers developed the proactive envelope controller with real-time road friction estimation, which can keep the vehicle within a stable region. But it still cannot certainly prevent the vehicle from veering away from the desired path when the road condition changes intensively.

Existing research has shown that appropriate longitudinal velocity planning is vital when following a path with tight curvature change [3]. The idea is to reduce vehicle speed before a potentially dangerous situation is reached, in contrast with widely used stability control systems that only react once loos of control is imminent. The insight is that the vehicle could have a larger stable operating region to follow the desired path with a smaller velocity [4][5].

However, they only consider the variation of curvature for longitudinal planning, and little attention has been paid to the road surface friction condition changing when conducting longitudinal velocity planning. For example, if the vehicle can preview the path friction reduction and slow down appropriately before entering the slick region, then a complicated algorithm is not necessary to stabilize the vehicle. The prior estimation of friction and peak tire force, before the slick region is reached, allows a vehicle chassis control system to work more reliably and proactively [2]. As a result, even a normal steering control algorithm can enable the vehicle to follow the path well.

Unfortunately, it is almost impossible to preview the large area road condition just through the intelligence of individual vehicle, where each vehicle itself constantly measuring and navigating the world using in-vehicle system. A potential solution to preview the road surface friction condition is motivated by the increasing research into the cyber-physical system, especially Connected and Autonomous Vehicles (CAV). This solution takes advantage of network intelligence instead of individual intelligence, where the pre-measured road friction information from the individual vehicle is shared within the network. Within the network, the information can flow between vehicle to vehicle, vehicle to infrastructure, and vehicle to database systems. In this way, each vehicle and the roadside unit can measure local road friction [6][7] and share it with the cloud database. Each vehicle in the network can query the aggregated friction information from the shared

*Research supported by NSF.

Liming Gao is a graduate student in Mechanical Engineering at The Pennsylvania State University, University Park, PA 16803, USA (e-mail: lug358@ psu.edu).

Craig Beal is with Department of Mechanical Engineering, Bucknell University, Lewisburg, PA 17837, USA (e-mail: cbeal@bucknell.edu)

Daniel Fescenmyer is a undergraduate student in Mechanical Engineering at The Pennsylvania State University, University Park, PA 16803, USA (e-mail: dzf5248@psu.edu).

Sean Brennan is with the Department of Mechanical Engineering, The Pennsylvania State University, University Park, PA 16803, USA (e-mail: snb10@psu.edu). IEEE Member.

database. A demo framework of this network is shown in Fig. 1.

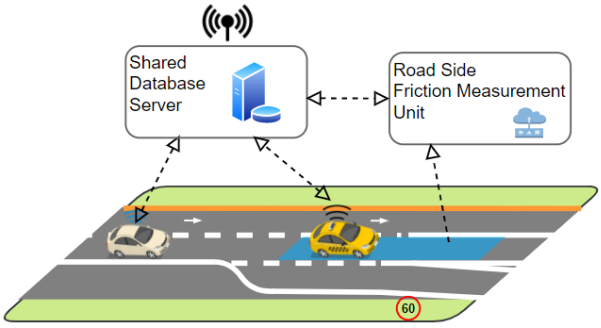

Figure 1. A strategy of road friction preview with a shared roadway database. (make the road curvy) The database can leverage shared intelligence to substantially improve the operation of each individual in the population.

The improvements in vehicle safety can be achieved by limiting the vehicle speed based on the road condition. In this paper, an idea of road friction preview through database-informed CAV is introduced. Then inspired by the work in DDL on vehicle dynamics at the limits of handing [8]–[10], we present an algorithm to generate a longitudinal vehicle velocity limit profile for a given desired path with the preview of path friction. Moreover, relationships are established between data confidence, preview distance, and vehicle speed for a vehicle traversing a roadway system augmented with such a preview system.

The remainder of this paper is organized as follows: Section II discusses the velocity limit profile planning based on the tire limits. Section III analyzes the preview distance. Section IV shows an application case. Finally, a conclusion section summarizes the main results of the work.

II. Vehicle Longitudinal Velocity Planning Given a Reference Path

This section presents the generation of limit speed profile which vehicles can achieve without exceeding available tire friction limits constraints [11]. At first, the longitudinal dynamic driving on the friction circle is derived, and then introduce the approach to describe the path by station s, curvature κ and friction coefficient. Finally, show the detailed velocity planning method.

A. Vehicle Chassis Model and Tire Friction Limits

The vehicle dynamic equations for the three states single track model shown in Fig. 2 are:

$$\dot{U}_x = \frac{F_{xf}\cos(\delta) - F_{yf}\sin(\delta) + F_{xr}}{m} + rU_y - g\sin(\theta) \quad (1)$$

$$\dot{U}_y = \frac{F_{yf}\cos(\delta) + F_{xf}\sin(\delta) + F_{yr}}{m} - rU_x \quad (2)$$

$$\dot{r} = \frac{a(F_{yf}\cos(\delta) + F_{xf}\sin(\delta)) - bF_{yr}}{I_{zz}} \quad (3)$$

where longitudinal velocity U_x, lateral velocity V_y and yaw rate r are the three states. θ is the path grade, and g is the gravitational acceleration. The vehicle parameters include the vehicle's mass m, yaw moment of inertia I_{zz}, front wheel steering angle δ, and a and b the distance from the vehicle's center of gravity to the front and rear axle respectively. Forces F_{xf}, F_{yf}, F_{xr}, F_{yr} are the forces acting on the front and rear tires.

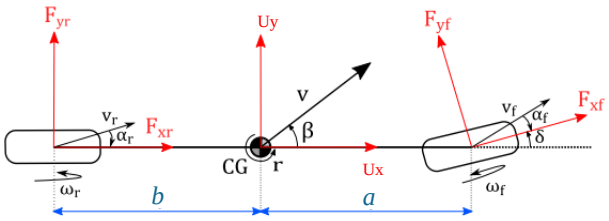

Figure 2. Planar single-tack vehicle chasis model (need a high resolution version and the direction of af and ar is wrong. v⟶ U)

The available longitudinal force F_x and lateral force F_y at each tire is constrained by friction circle:

$$F_{xf}^2 + F_{yf}^2 \le \left(\mu F_{zf}\right)^2 \quad (4)$$

$$F_{xr}^2 + F_{yr}^2 \le \left(\mu F_{zr}\right)^2 \quad (5)$$

where μ is the road-tire friction coefficient, and F_{zf} and F_{zr} are the normal force at the front and rear axle respectively. If ignore the load transfer, the normal forces are $F_{zf} = bmg/(a+b)$, $F_{zr} = amg/(a+b)$.

Determining the limit speed profile requires the vehicle to utilize all the available tire friction to generate forces so that vehicle can operate at acceleration limits to achieve the maximum safe speed [12]. It implies that all tire forces need to remain on the boundary of the friction circle:

$$F_{xf}^2 + F_{yf}^2 = \left(\mu F_{zf}\right)^2 \quad (6)$$

$$F_{xr}^2 + F_{yr}^2 = \left(\mu F_{zr}\right)^2 \quad (7)$$

Fig. 3 shows the tire force when maneuvering through a left corner of a path. The boundary of the friction circle depends on the road-tire friction coefficient.

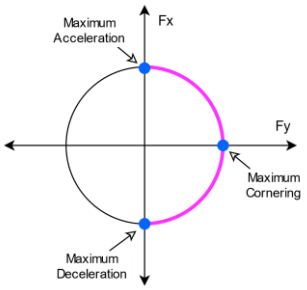

Figure 3. The maximum performance of vehicle can be achieved by driving at the boundary of friction circle. This plot shows the left cornering case.

As this work is interested in the longitudinal dynamic, assume the lateral states are steady:

$$\dot{V}_y = 0, \quad V_y = 0, \quad \dot{r} = 0, \quad r = \kappa U_x \tag{8}$$

where κ is the path curvature.

Substituting (6), (7), and (8) into (1), (2), and (3) yields:

$$\dot{U}_x = \pm\sqrt{(\mu g)^2 - \left(\kappa U_x^2\right)^2} - g\sin(\theta) \tag{9}$$

Before going further, an adjusting parameter λ is added into the equation (9) for two reasons: a. compensation for the uncertainty of friction preview; b. common driver may not able to operate a vehicle at friction limit as racecar drivers or autonomous driving systems [13]. Consequently, the dynamics equation that depicts the maximum available longitudinal acceleration is expressed as:

$$\dot{U}_x = \pm\sqrt{(\lambda\mu g)^2 - \left(\kappa U_x^2\right)^2} - g\sin(\theta) \tag{10}$$

where the plus-minus sign (±) corresponds to acceleration and deceleration respectively. Positive θ is for upgrades and negative is for downgrades. The parameters μ and κ in (9) depend on the path position. And the path description method is introduced in the following session.

B. Path Representation

This paper does not focus on path planning. Therefore, the desired path is assumed to be given. The clothoid path description is widely used for highway road design [14] and vehicle path planning, for example, the racing line [10], [15] and minimum curvature optimal path [16] [17]. A clothoid path can generally be described by a succession of turns - consist of spirals and constant radius arcs - and straight lines. The curvature of the spiral is linearly increasing along with the distance:

$$\kappa = (\kappa_c / L_s)s \tag{11}$$

where s called "station" in this paper is the distance measured along a path; L_s is the total length of the spiral and κ_c is the curvature at the end of the spiral. In this way, the curvature of the whole path can be described by a succession of linear functions.

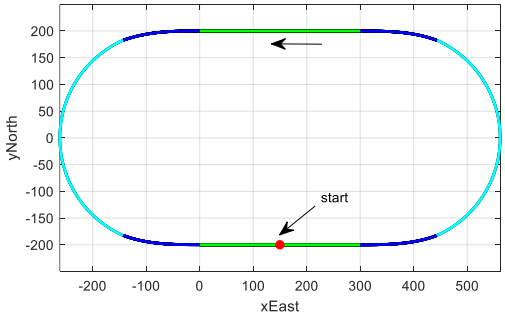

Figure 4. A circular oval smaple path. (update to a real oval).

Without loss of generality, an example oval path similar to the Larson Institute Test Track [18] is shown in Fig. 4. The path is given according to the highway road design rule which decomposes the cornering into three phases: an entry clothoid ~~for trail braking~~, a circle arc ~~for pure cornering~~, and an exit clothoid ~~for throttle exit~~ [10]. The curvature and previewed friction coefficient and grade are shown in Fig. 5. All of these path parameters can be described as a function of the path station: κ(s), μ(s), θ(s). The example path where the grade is not zero is similar to the off-ramp and on-ramp part of a highway.

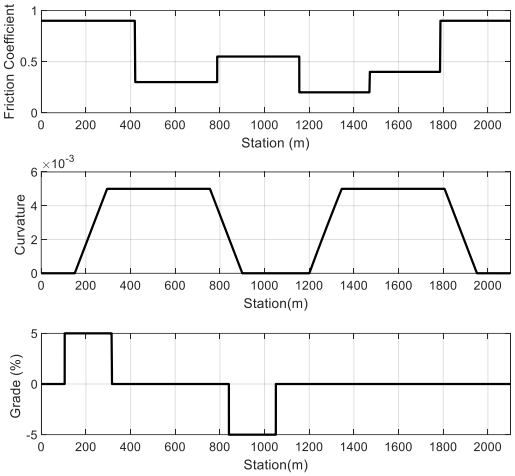

Figure 5. The curvature, previewed friction coefficient, and previewed grade for sample path. The friction is assumed to change abruptly.

C. Velocity Profile Generation

Velocity planning has a significant impact on driving safety, especially when vehicles drive on a road with changing friction and geometry. With the longitudinal dynamic equation (9) and the desired path description, the speed profile can be determined. The approach presented in this paper is inspired by those works: three passes [11], nonlinear optimization [3], segment and iteration [19], where a velocity profile is planned given the path curvature.

Express the longitudinal acceleration with respect to the station:

$$\dot{U}_x = \frac{dU_x}{dt} = \frac{dU_x}{ds}\frac{ds}{dt} = \frac{dU_x}{ds}U_x \tag{12}$$

Substitute (12) into (10) yields:

$$\frac{dU_x(s)}{ds} = \frac{1}{U_x(s)}\left(\pm\sqrt{(\lambda\mu(s)g)^2 - \left(\kappa(s)U_x^2(s)\right)^2} - g\sin(\theta(s))\right) \tag{13}$$

(13) can be solved using a numerical integration method as a general analytical solution cannot be found for all cases.

$$U_x(s_{k+1}) \approx U_x(s_k) + \frac{\Delta s}{U_x(s_k)}\left(\pm\sqrt{(\lambda\mu(s_k)g)^2 + \left(\kappa(s_k)U_x^2(s_k)\right)^2} - g\sin(\theta(s_k))\right) \tag{14}$$

where $\Delta s = s_{k+1} - s_k$. The solution will be accurate enough if path waypoints are dense, i.e. the Δs is small enough. In this paper, we choose Δs smaller than 0.1m. λ=0.95 is taken.

The first step of generating the speed profile is to find the maximum permissible steady-state vehicle velocity with zero longitudinal acceleration, which is given by (15):

$$U_x(s) = \sqrt{\mu(s)g / \kappa(s)} \tag{15}$$

Notice that the steady-state speed will be very high when the curvature is small (the curvature is zero for a straight line) and thus a speed limit of 55m/s was imposed. The first step result is shown as the "curve limit speed" in Fig. 6(a).

The following next step is a forward integral step:

$$U_x(s_{k+1}) \approx U_x(s_k) + \frac{\Delta s}{U_x(s_k)}\left(\sqrt{(\lambda\mu(s_k)g)^2 + \left(\kappa(s_k)U_x^2(s_k)\right)^2} - g\sin(\theta(s_k))\right) \quad (16)$$

It starts from the vehicle's current speed. At each step, the result is compared to the curve limit speed, and the minimum value is taken. This step indicates how fast a vehicle can accelerate.

The final step is a backward integral step:

$$U_x(s_{k+1}) \approx U_x(s_k) - \frac{\Delta s}{U_x(s_k)}\left(\sqrt{(\lambda\mu(s_k)g)^2 + \left(\kappa(s_k)U_x^2(s_k)\right)^2} + g\sin(\theta(s_k))\right) \quad (17)$$

It starts from the maximum allowable vehicle speed at the end of the path and back toward to current station. At each step, the result is compared to the forward integral results. This step indicates how fast a vehicle can decelerate.

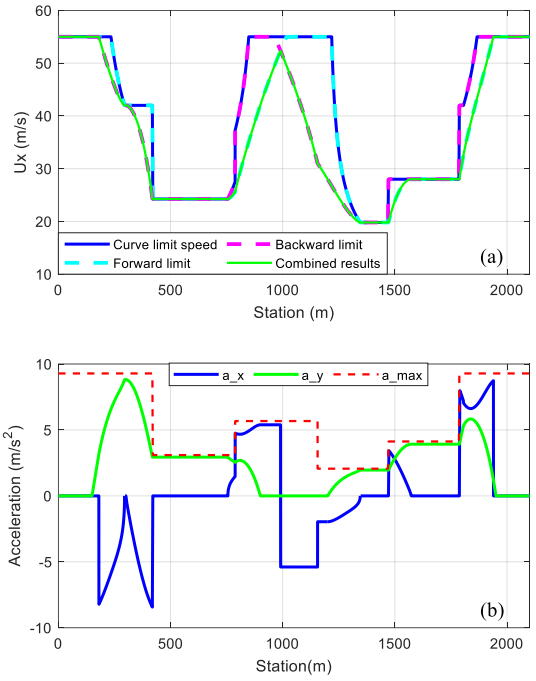

Figure 6. (a) The intermediate and final results of the speed profile of the computation algorithm. (b) The acceleration of the speed profile.

The speed profile results and the acceleration for the example path are shown in Fig. 6. Note that from Fig. 6 (b), the acceleration value is relatively large as a racing car especially at the large friction region, but the acceleration value can be tailored by choosing a proper adjusting parameter λ.

III. Preview Distance

When a vehicle query friction preview from a shared database, a tradeoff problem is to determine a proper preview distance. The longer preview distance involves more data transmitting which results in more time delay and data cost, but with a shorter preview distance, a vehicle could not have enough space to respond to the dangerous situation ahead. Therefore, this section presents a way to determine the minimum friction preview distance for a zero grade case so that a vehicle can have sufficient time to take action for upcoming hazardous situations.

A. Minimum Friction Preview Distance

The criterion for determining the preview distance in this paper is that a vehicle could always stop within the distance. The strategy is to calculate the maximum stop distance with the most critical scenario for conservation. Therefore, we assume that the vehicle is driving on a snowy road with a constant road-tire friction coefficient value, i.e. λμ=0.2, and with a maximum permissible initial speed. With this assumption, our task is to find the scenario where the vehicle decelerates to stop with the longest distance.

Section II.B indicates that a path comprises straight lines with zero curvature, radius arcs with constant curvature, and spirals with linear curvature. Thus, for a given path, the straight-line segment could allow the most permissible initial speed. According to (13), the path with larger curvature has a smaller maximum permissible initial speed. And for a given initial speed, a larger curvature path results in a smaller deceleration and thereby a longer stop distance. With this analysis, the most critical scenario is that a vehicle driving at the speed limit U_{x0} at a straight-line road, then enter a spiral road, and finally stop at the arc segment, which is pretty similar to a highway off-ramp road and is shown as Fig. 7.

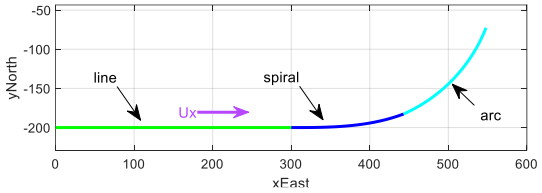

Figure 7. The scenario where a vehicle decelerates starts from a line segment with an initial speed Ux0, then enters a piral segment with length L_s, and finally stops at the arc segment with radius $R_c=1/\kappa_c$. (add Ls and Rc label, off rampe turn, leaving the road boundary will crash)

Now the task is to analyze the deceleration behavior at each path segment of Fig. 7.

For the line segment path whose curvature is zero, the deceleration distance can be determined by solving (13) analytically:

$$d_{s\_l} = \left(U_{x0}^2 - U_{x\_lf}^2\right) / 2\lambda\mu g \quad (18)$$

where U_{x_lf} is the final velocity of the line segment and the initial velocity of the spiral segment, which can be determined as follows.

For the spiral path, we suppose its length is:

$$L_s \quad (19)$$

Then the numerical solution of U_{x_lf} can be derived from (13):

$$U_x(s_{k+1}) \approx U_x(s_k) + \frac{\Delta s}{U_x(s_k)}\sqrt{(\lambda\mu(s_k)g)^2 + \left(\kappa(s_k)U_x^2(s_k)\right)^2} \quad (20)$$

for $k = 0,1,2,3, \ldots, N = L_s/\Delta s$, where $\kappa(s_k) = (\kappa_c / L_s)s_k$, and $s_0 = L_s$, $U_x(s_N) = U_{x\_lf}$, and $U_x(s_0) = U_{x\_a0}$ is the initial speed of arc path segment, which is determined as follows.

For the radius arc path whose curvature is a constant, the stop distance can be determined by solving (13) analytically:

$$d_{s\_a} = \frac{1}{2\kappa_c} \tan^{-1} \frac{U_{x\_a0}^2}{\sqrt{(\mu g / \kappa_c)^2 - U_{x\_a0}^4}} \tag{21}$$

(21) implies that the stop distance is increasing with the increase of U_{x0}, but d_{s_a} has a supremum when $U_{x\_a0} = \sqrt{\mu g / \kappa_c}$:

$$d_{s\_a,\sup} = \frac{\pi}{4\kappa_c} = \frac{\pi R_c}{4} \approx R_c \tag{22}$$

The supremum is independent of friction μ, and the reason is that the initial speed on the circular arc is limited by curvature and friction.

The total stop distance is the addition of (18), (19), and (22):

$$d_s = d_{s\_l} + L_s + d_{s\_a,\sup} \tag{23}$$

With a range of reasonable values of κ_c and L_s following the highway design rules[14], for a fixed value of U_{x0}, we can determine the relationship between the total stop distance (23) and κ_c, L_s, which is shown in Fig. 8.

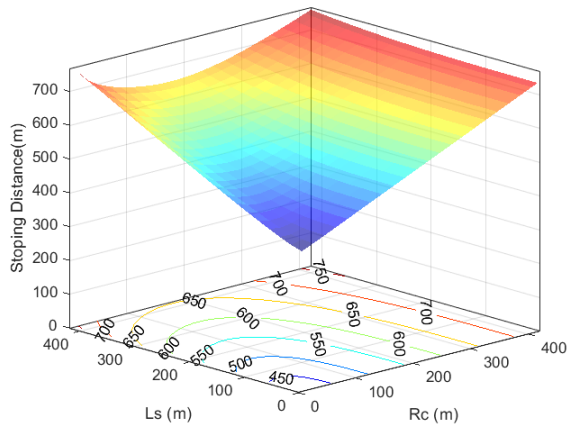

Figure 8. The stopping distance on entering clothoid path with an initial speed U_{x0} = 40m/s. In this plot, $R_c = 1/\kappa_c$.

Fig. 8 indicates that the longest stop distance is achieved when R_c, L_s are relatively large. Look at it quantitatively the maximum stopping distance is less than 750m if the L_s is less than 400m and R_c is less than 400 m. This conclusion works for all initial speeds less than the speed limit of 40m/s.

More precisely, the preview distance can be calculated using (23) given vehicle initial speed U_{x0}, path parameters: $\kappa_{c,\min}$ and L_{s_max}, assumed minimum friction coefficient $\mu_{\min}$, and a conservative constant c.

$$d_{prev} = f(\kappa_{c,\min}, L_{s,\max}, \mu_{\min}, U_{x0}, c) \tag{24}$$

For the example path in this paper, the minimum preview distance is 790m.

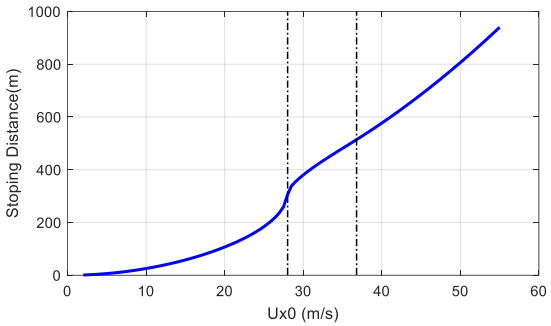

Figure 9. The stoping distance on entering clothoid path with different initial speed. In this plot, R_c = 400m and L_s = 200m.

Most human drivers with the required driving vision can only see the road approximately 500m ahead even on a clear day when driving [ref]. Unfortunately, the visibility reduces a lot during darkness and adverse weather, such as fog, rain, and snow, where dangerous road condition occurs. Besides, the driver's sight is limited at path corners and hills. Thus, the preview of road friction could help a lot for the driver to take action proactively.

IV. Application Case and Simulation Results

A vehicle with rear driving, front steering, understeering or oversteering.

For the sample path, compares the velocity results considering only curvature and the results considering both friction and curvature.

A simple driver controller (look ahead error method which is similar to the human driver may need to find a reference) can follow the path well with the preview of friction.

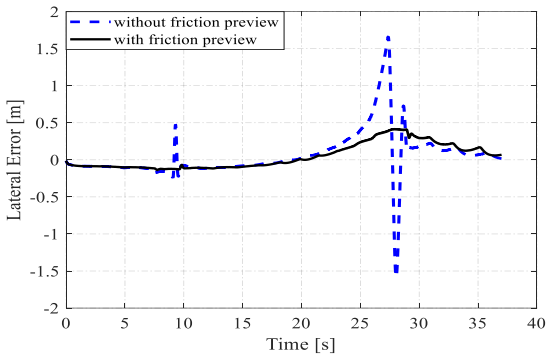

Figure 9. The lateral error betwee different preview: constant speed, with curvature preview, with friction preview

V. Conclusion and Future Work

In this paper, we present a method for planning longitudinal speed profiles for CAVs that have previewed information about road geometry and friction conditions. The idea of preview is to extend individual intelligence with network intelligence. The longitudinal speed planning is to develop an analytical solution to the allowable velocity profile that prevents departure from the friction ellipse. The results further define the relationship between the minimum preview distance and longitudinal velocity limits that ensure the vehicle has sufficient time to take action for upcoming hazardous situations. The efficacy of the algorithm is demonstrated through an application case where a vehicle is navigating curvy roads with changing friction conditions at maximum speeds, with results showing that the vehicle consistently operates within the available friction limits.

For the preview distance, this paper just presents the most conservative results. In the future, a more precise and dynamic preview distance can be analyzed. Also, the paper does not talk about the friction split case. Besides, it is worth exploring the speed profile dependency on the preview distance because intuitively the vehicle needs to move slower if with less visibility.

Acknowledgment

This material is based upon work supported by the National Science Foundation under grant no. CNS-1932509 CNS-1931927, CNS-1932138 “CPS: Medium: Collaborative Research: Automated Discovery of Data Validity for Safety-Critical Feedback Control in a Population of Connected Vehicles”.

References

L. Yu, S. Zheng, Y. Dai, L. Abi, X. Liu, and S. Cheng, “A feedback-feedforward steering controller designed for vehicle lane keeping in hard-braking manoeuvres on split-μ roads,” *Veh. Syst. Dyn.*, 2021, doi: 10.1080/00423114.2020.1869274.

L. Li, “PID PLUS FUZZY LOGIC METHOD FOR TORQUE CONTROL IN TRACTION CONTROL SYSTEM,” *Int. J. Automot. Technol.*, vol. 13, no. 3, pp. 441–450, 2012, doi: 10.1007/s12239.

H. Cao, X. Song, S. Zhao, S. Bao, and Z. Huang, “An optimal model-based trajectory following architecture synthesising the lateral adaptive preview strategy and longitudinal velocity planning for highly automated vehicle,” *Veh. Syst. Dyn.*, vol. 55, no. 8, pp. 1143–1188, 2017, doi: 10.1080/00423114.2017.1305114.

C. E. Beal and C. Boyd, “Coupled lateral-longitudinal vehicle dynamics and control design with three-dimensional state portraits,” *Veh. Syst. Dyn.*, vol. 57, no. 2, pp. 286–313, 2019, doi: 10.1080/00423114.2018.1467019.

C. G. Bobier-Tiu, C. E. Beal, J. C. Kegelman, R. Y. Hindiyeh, and J. C. Gerdes, “Vehicle control synthesis using phase portraits of planar dynamics,” *Veh. Syst. Dyn.*, vol. 57, no. 9, pp. 1318–1337, 2019, doi: 10.1080/00423114.2018.1502456.

[6] S. Roychowdhury, M. Zhao, A. Wallin, N. Ohlsson, and M. Jonasson, “Machine Learning Models for Road Surface and Friction Estimation using Front-Camera Images,” in *2018 International Joint Conference on Neural Networks (IJCNN)*, 2018, pp. 1–8, doi: 10.1109/IJCNN.2018.8489188.

[7] C. E. Beal, “Rapid Road Friction Estimation using Independent Left/Right Steering Torque Measurements,” *Veh. Syst. Dyn.*, vol. 58, no. 3, pp. 377–403, 2020, doi: 10.1080/00423114.2019.1580377.

[8] J. Subosits and J. C. Gerdes, “Autonomous vehicle control for emergency maneuvers: The effect of topography,” *Proc. Am. Control Conf.*, vol. 2015-July, pp. 1405–1410, 2015, doi: 10.1109/ACC.2015.7170930.

[9] K. Kritayakirana and J. C. Gerdes, “Autonomous vehicle control at the limits of handling,” *Int. J. Veh. Auton. Syst.*, vol. 10, no. 4, pp. 271–296, 2012, doi: 10.1504/IJVAS.2012.051270.

[10] P. A. Theodosis and J. C. Gerdes, “Nonlinear optimization of a racing line for an autonomous racecar using professional driving techniques,” in *ASME 2012 5th Annual Dynamic Systems and Control Conference Joint with the JSME 2012 11th Motion and Vibration Conference, DSCC 2012-MOVIC 2012*, 2012, vol. 1, pp. 235–241, doi: 10.1115/DSCC2012-MOVIC2012-8620.

[11] N. R. Kapania, J. Subosits, and J. C. Gerdes, “A Sequential Two-Step Algorithm for Fast Generation of Vehicle Racing Trajectories,” *J. Dyn. Syst. Meas. Control. Trans. ASME*, vol. 138, no. 9, 2016, doi: 10.1115/1.4033311.

[12] W. C. Mitchell, R. Schroer, and D. B. Grisez, “Driving the traction circle,” *SAE Tech. Pap.*, no. 724, 2004, doi: 10.4271/2004-01-3545.

[13] C. E. Beal and J. C. Gerdes, “Model predictive control for vehicle stabilization at the limits of handling,” *IEEE Trans. Control Syst. Technol.*, vol. 21, no. 4, pp. 1258–1269, 2013, doi: 10.1109/TCST.2012.2200826.

[14] AASHTO, *A Policy on Geometric Design of Highways and Streets*. 2018.

[15] P. A. Theodosis and J. C. Gerdes, “Generating a racing line for an autonomous racecar using professional driving techniques,” *ASME 2011 Dyn. Syst. Control Conf. Bath/ASME Symp. Fluid Power Motion Control. DSCC 2011*, vol. 2, pp. 853–860, 2011, doi: 10.1115/DSCC2011-6097.

[16] J. Villagra, V. Milanés, J. Pérez, and J. Godoy, “Smooth path and speed planning for an automated public transport vehicle,” *Rob. Auton. Syst.*, vol. 60, pp. 252–265, 2012, doi: 10.1016/j.robot.2011.11.001.

[17] H. A. Hamersma and P. S. Els, “Longitudinal vehicle dynamics control for improved vehicle safety,” *J. Terramechanics*, vol. 54, pp. 19–36, 2014, doi: 10.1016/j.jterra.2014.04.002.

[18] “Test Track.” https://www.larson.psu.edu/about/test-track.aspx (accessed Apr. 08, 2021).

[19] R. Solea and U. Nunes, “Trajectory planning with velocity planner for fully-automated passenger vehicles,” *IEEE Conf. Intell. Transp. Syst. Proceedings, ITSC*, pp. 474–480, 2006, doi: 10.1109/itsc.2006.1706786.